The anti-apoptotic Mcl-1 protein controls the type of cell death in Theiler's virus-infected BHK-21 cells

Sevim Yildiz Arslan, M.S., Kyung-No Son, Ph.D., and Howard L. Lipton, M.D.

Department of Microbiology-Immunology, University of Illinois at Chicago, Chicago, IL

Abstract = 253

Word count: Text =

References =

Running title: Mcl-1 controls Theiler's virus-induced cell death

Keywords: Theiler's virus, apoptosis, Mcl-1, necrosis

Send correspondence to HLL:

Department of Microbiology and Immunology, MC 790

University of Illinois at Chicago

835 South Wolcott

Chicago, IL 60612-7344

Phone: 312-996-5754

Email: hlipton@uic.edu

Conflict of interest statement:

ABSTRACT

Theiler's murine encephalomyelitis virus (TMEV) is a highly cytolytic RNA virus that produces a persistent central nervous system infection and immune-mediated demyelination in susceptible strains of mice. TMEV-infected macrophages (mϕs) undergo apoptosis which reduces the yield of infectious progeny (<10 pfu/cell), whereas TMEV infection of other rodent cells *in vitro*, e.g. baby hamster kidney cells (BHK-21), produces a canonical necrotic cytopathic effect with high virus yields (200-500 pfu/cell). In this study, we found that while most TMEV-infected BHK-21 cells became necrotic, ~20% of cells underwent apoptosis. Mcl-1, an anti-apoptotic Bcl-2 family member, was highly expressed in BHK-21 cells, but levels decreased upon infection, consistent with the onset of apoptosis. Infection in BHK-21 cells in which Mcl-1 expression was knocked down using silencing (si) RNA that an ~ 3-fold increase in apoptotic cell death compared to that in parental cells. Infection of stable Mcl-1-knock-down cell lines led to restricted viral titers, unlike the high viral titers observed in parental cells. The apoptotic program switched on by TMEV replication appeared to be similar to that in mouse M1-D mϕs, with hallmarks of activation of the intrinsic apoptotic pathway in a tumor suppressor protein p53-dependent manner. Subsequent activation of the Bcl-2 BH-only pro-apoptotic Noxa protein led to degradation of Mcl-1, activation of Bax and cleavage of caspases-9 and -3. Together, these results indicate that Mcl-1 acts as a critical pro-survival factor that protects against apoptosis in a p53-dependent manner and restricts the production of infectious virus in BHK-21 cells.

INTRODUCTION

Theiler's murine encephalomyelitis viruses (TMEV), members of the *Cardiovirus* genus in the family *Picornaviridae*, are enteric pathogens of mice and. TMEV strains differ in neurovirulence following intracerebral inoculation of mice with the high-neurovirulence GDVII strain causing an extensive infection of neurons in the cerebral cortical and hippocampus neurons, and producing a rapidly fatal encephalitis, whereas low-neurovirulence DA and BeAn strains result in a persistent central nervous system (CNS) infection primarily in microglia/macrophages (mϕs) but also in oligodendrocytes, leading to immune-mediated demyelination. TMEV persistence in mice is recognized as a relevant experimental animal model for multiple sclerosis (4, 15).

Depending on the specific cell type infected, TMEV induces at least two distinct cell death programs, canonical necrosis and apoptosis, which result in substantial differences in infectious viral yields. All rodent cell types except for mϕs appear to undergo necrosis because of the high viral yields (14); murine mϕs undergo apoptosis with restricted viral yields, producing only a few plaque-forming units (pfu) of virus per cell (13). Moreover, TMEV infection of mouse M1-D mϕs induces apoptosis by activating the intrinsic apoptotic pathway (13, 27). In those cells, TMEV infection reportedly results in activation of p38 mitogen-activated protein kinase by 2-3 h post-infection (pi), followed by phosphorylation of tumor suppressor protein p53 Ser 15 at 3 to 6 h pi and stable p53 levels until 6 h pi; activated p53 up-regulates the transcription of the pro-apoptotic *puma* and *noxa* genes at 2 to 4 h pi, and levels of pro-survival Mcl-1 and A1 proteins become undetectable at 4 to 10 h pi (27, 28). Specific inhibition of phospho-p38 and inhibiton of p53 by a genetic suppressor element led to a significant decrease in apoptosis (28). Degradation of pro-survival proteins

was also shown to release Bax (27, 28), which forms homo-oligomers and translocates into and permeabilizes the mitochondrial outer membrane, releasing cytochrome c and initiating the caspase cascade

Anti-apoptotic Mcl-1, initially isolated from a human myeloblastic leukemia cell line (17), predominates in differentiated human mϕs (20), protecting against apoptosis during the initial steps of differentiation (7, 33). Overexpression of Mcl-1 in TMEV-infected M1-D cells reduced the cleavage of caspases-3 and -9 to their active forms and inhibited apoptosis (28). Whether Mcl-1 endogenously regulates TMEV-induced cell death in other cells remains to be determined.

In the present study TMEV infection in BHK-21 cells led to necrosis of the majority of cells, but to apoptosis in approximately 20% of cells through the intrinsic apoptotic pathway in a p53-dependent manner. Mcl-1, an anti-apoptotic Bcl-2 family member, was highly expressed in BHK-21 cells and infection resulted in gradual loss of Mcl-1, consistent with the onset of apoptosis. Mcl-1 knock-down by silencing (si) RNAs increased apoptotic cell death by ~3-fold, and concomitantly reduced infectious viral yields by at least 12-fold, indicating that Mcl-1 is an important regulator of cell death in infected BHK-21 cells. The availability of BHK-21 cells with stably knocked-down Mcl-1 expression provides a convenient tool to further define the step(s) in the viral life cycle impacted by apoptosis.

MATERIALS AND METHODS

Cells and viruses. BHK-21 cells were grown in Dulbecco's modified Eagle medium supplemented with 10% fetal bovine serum (FBS), 7.5% tryptose phosphate, 2 mM L-glutamine, 100 U/ml penicillin, and 100 μg/ml streptomycin at 37°C in 5% CO_2. Cells of the immature myelomonocytic cell line M1, derived from the SL mouse strain, were induced to differentiate into mϕs with supernatants from mouse L929 fibroblasts and mouse P388D1 mϕs as described (27). N20.1 mature mouse oligodendrocytes were grown in Dulbecco's modified Eagle medium-F12 medium containing 100 μg of streptomycin and 100 U of penicillin per ml and 10% FBS at 37°C in 5% CO_2. The origin and passage history of the BeAn virus stock has been described (25). Virus titers of clarified lysates of infected cells were determined by standard plaque assay in BHK-21 cells (25).

Reagents. The following reagents and antibodies were purchased commercially: mouse anti-caspase 9, rabbit anti-caspase 3, rabbit anti-poly(ADP-ribose) polymerase (PARP), and rabbit anti-actin antibodies (Cell Signaling Technology, Beverly, MA USA); mouse anti-Bax, Mcl-1 siRNA and Mcl-1 short hairpin (sh)RNA (Santa Cruz Biotechnology Inc., Santa Cruz, CA, USA); goat anti-mouse IgG-horseradish peroxidase and goat anti-rabbit IgG-horseradish peroxidase (BD Pharmingen, San Diego, CA USA); and actinomycin D (Sigma, St. Louis, MO USA).

Virus infections. After virus adsorption at a multiplicity of infection (moi) of 10 for 45 min at 24°C, cell monolayers were washed twice with phosphate-buffered saline (PBS) containing 1 mM $CaCl_2$ and 0.5 mM $MgCl_2$ and incubated in Dulbecco's modified Eagle medium containing 1% FBS at 37°C for designated times. The end of the adsorption period

was designated as time zero.

Fluorescence-activated cell sorting (FACS). Subconfluent monolayers of BHK-21 cells in 35-mm 6-well plates were infected with BeAn virus (moi = 10) for 16 or 24 h; in some experiments this was after transfection with Mcl-1 siRNAs for 24 h. Cell monolayers were washed with PBS, detached with trypsin, and 5 x 10^5 cells were stained with propidium iodide (PI) and Annexin V-fluorescein isothiocyanate (Calbiochem, Darmstadt, Germany) according to the manufacturer's instructions. Incubation of cell monolayers with actinomycin D (3 μg/ml) provided positive controls for apoptosis. For each sample, 10,000 events were analyzed using a Beckman Coulter Epics Elite ESP and FlowJo 8.8.3 software.

Viral titers. Cell monolayers (2 x 10^4 cells/well) in 96-well plates were infected with serial 10-fold dilutions of virus, and viral cytopathic effect (cpe) was monitored under an inverted light microscope. On day 5 of incubation, the $TCID_{50}$ ml^{-1} was calculated as the reciprocal of the lowest 10-fold dilution resulting in cpe in more than 50% of monolayers (23).

Cell viability assay. WST-1 reagent (Roche Applied Science, Indianapolis, IN, UDA), a tetrazolium salt, was added to the medium of monolayer cultures in 96-well plates at indicated times and incubated for 1 to 2 h at 37°C in 5% CO_2. Cell viability in samples was determined by absorbance at 420 nm (reference wavelength, 610 nm) for cleavage of the tetrazolium salt to formazan against a background control using a Vmax kinetic microplate reader (Molecular Devices, Sunnyvale, CA USA). Percent cell death values were calculated as the ratio of BeAn virus-infected to mock-infected cultures.

Apoptosis assay. The number of apoptotic cells was determined using DAPI staining. Briefly, M1-D cells grown and infected on glass coverslips (Fisher Scientific Co., Pittsburgh, PA, USA) were fixed in 4% paraformaldehyde for 15 min at room temperature, washed twice in PBS (pH 7.2), and incubated with DAPI for 5 min at a final concentration of 0.5 µg/ml. Coverslips were washed with 0.5% Tween 20 in PBS and distilled H_2O and viewed with a Zeiss digital confocal microscope. At least three randomly chosen fields containing cells were photographed at ×200 magnification, and the percentage of cells with condensed chromatin and fragmented nuclei were determined by a blinded observer; each experiment was repeated twice.

Caspase activity assay. Caspase-8 and -9 activities were assayed with Caspase-Glo reagent (Promega, Madison USA) in BHK-21 cells seeded in 6-well plates (3×10^5 cells per well), infected 24 hr later with BeAn virus (moi = 10) and harvested at 12 pi. An equal volume of Caspase-Glo reagent containing MG132 was added to infected cell pellets which were transferred to white-walled 96-well plates, incubated at room temperature for 1 h, and luminescence measured in a plate-reading luminometer (GloMax®-multi detection system (Promega).

Assay for reactive oxygen species (ROS). Cellular ROS production was measured by flow cytometry using the ROS-sensitive dye 5- (and 6-)chloromethyl-2',7'-dichlorodihydrofluorescein diacetate, acetyl ester (CM-H_2DCFDA) (Molecular Probes, Eugene, Oregon, USA). Infected BHK-21 cells (12 h pi) were incubated with infection media containing 5 µmol/L CM-H_2DCFDA for 30 min in the dark at 37°C before harvesting.

Cells were trypsinized, washed with DMEM without pyruvate X2, suspended in 0.5 ml PBS and subjected to flow cytometry.

Northern hybridization. Total RNA from cell cultures was ethanol-precipitated, resuspended in RNA loading buffer (MOPS buffer), heated for 5 min at 95°C, and electrophoresed in a 1.2% agarose gel at 85 V for 2 h. The gel was soaked in 10X SSC for 15 min. RNA was passively transferred to a Hybond-N+ membrane (Amersham, Piscataway, NJ, USA), treated with short-wavelength UV light for 2 min and prehybridized with hybridization solution (Clontech, Mountain View, CA, USA) for at least 1 h at 68°C. A random-primed DNA probe specific for BeAn virus was derived from a 1.5-kb *BclI/NciI* fragment of BeAn cDNA spanning nucleotides 4952 to 6492 by using the Prime-a-gene Labeling System (Promega). The [α-^{32}P]-labeled probe was added to the prehybridization solution and hybridization was carried out overnight at 42°C. Membranes were washed once with 2X SSC-0.05% sodium dodecyl sulfate (SDS) for 30 min and three times with 0.1X SSC-0.1% SDS at 24°C for 20 min each time, dried, and exposed to a Molecular Dynamics PhosphorImager screen to detect BeAn virus with the [α-^{32}P]dNTP-labeled hybridized probe.

Pulse-labeling virus proteins. Cell monolayers were infected with BeAn (moi = 50) for 4 h with infection medium containing 2 µg/ml actinomycin D. After rinsing, cells were incubated with methionine-free DMEM and 2 µg/ml Actinomycin D for 1 h followed by incubation for 5 min in medium containing 30 μCi of [^{35}S] methionine. Cells were rinsed and chased in the presence of 10 mM methionine for 0, 1, 5, 10 and 20 min. Next, cells were harvested, lysed with 0.1 ml of lysis buffer [1% NP-40, 0.5% Na-deoxycholate, 0.1% sodium

deoxycholate, 150 mM NaCl, 1 mM EDTA, 50 mM Tris (pH 7.5)] and centrifuged at 13,000 rpm for 20 min at 4°C. Aliquots were analyzed by SDS-12% polyacrylamide gel electrophoresis (PAGE), followed by autoradiography.

Electron microscopy. M1-D cells were harvested and fixed with 3% glutaraldehyde in PBS and then in aqueous 2% osmium tetroxide, stained with 0.5% aqueous uranyl acetate, dehydrated with a graded ethanol series and embedded in Epoxy Resin LX112 for processing and staining as described (27).

Statistical analysis. Paired Student's *t*-test was used to compare groups; and differences were considered significant at $p < 0.05$.

RESULTS

BeAn virus infection induces both necrotic and apoptotic cell death pathways in BHK-21 cells. Since TMEV infection of BHK-21 cells is highly productive, with infectious viral yields on the order of 200 to 500 pfu/cell (25), these cells have been widely used to purify the virus and study its molecular virology. Analysis of cell viability in BHK-21 cells infected with the BeAn strain of TMEV at (moi = 10) revealed progressive virus-induced cell death, with 85% of the cells dying by 24 h pi. (Figure 1A). FACS analysis revealed that cell death was due to a combination of necrosis and apoptosis (Figure 1B), with most cells dying by necrosis and ~20% by apoptosis at 24 h pi (Fig. 1C). Moreover, the very high levels of reactive oxygen species observed by 10 to 12 hr pi (Figure 1C) are consistent with necrosis since its production in cell death is thought to be higher in necrosis than apoptosis (9). Figure 1D shows representative electron micrographs of an almost normal-appearing

cell early in infection (left), and of necrotic (center) and apoptotic (right) cells at 16 h pi. The necrotic cell is swollen, with little recognizable cytoplasmic and nuclear architecture remaining; the apoptotic cell is slightly shrunken with condensed nuclear chromatin and blebbing of a part of its nucleus, and proliferative membranes or viroplasm in the cytoplasm where viral RNA replication occurs. Thus, infection of BHK-21 cells resulted primarily in necrosis, with only a minority of cells undergoing apoptosis.

Mcl-1 expression in BHK-21 and mouse cell lines. Based on the prominent anti-apoptotic role of Mcl-1 in BeAn virus-infected M1-D mϕs (27, 28), we examined Mcl-1 expression in mouse cells, including five mϕ and two fibroblast cell lines, and in BHK-21 cells. Immunoblotting analysis revealed low levels of Mcl-1 in the murine cells compared to abundant expression in the hamster-derived BHK-21 cells (Figure 2A). Because BHK-21 cell Mcl-1 consistently migrated above the mouse species in polyacrylamide gels, the nucleotide sequence was determined; Syrian hamster Mcl-1 has one less one amino acid smaller in size (319 amino acids) and shares 93% sequence identity with its mouse counterpart (GenBank accession number U35623). Assessment of the expression of the five Bcl-2 anti-apoptotic family members demonstrated abundant Bcl-xL expression in both BHK-21 and M1-D cell lines and Mcl-1 in BHK-21 cells, but minimal expression of the other anti-apoptotic proteins in BHK-21 cells (Figure 2B). Because Mcl-1 expression was abundant and might not be regulated, BHK-21 cells were maintained for 36 h in medium containing 0.1% FBS before immunoblotting; Mcl-1 expression decreased at 24 to 36 hr (Figure 2C), indicating that Mcl-1 is regulated by other signaling pathways, such as ERK (reviewed in 16). Following BeAn virus infection (moi = 10), Bcl-xL expression remained stable from 0 (end of adsorption period) to 12 h pi, while that of Mcl-1 decreased by >50%

at 10 to 12 h pi (Figure 2D,E). Assuming steady-state Mcl-1 synthesis and degradation, this decrease in Mcl-1 expression at 10 to 12 hr is consistent with the onset of apoptosis.

Mcl-1 is anti-apoptotic in BeAn virus-infected BHK-21 cells. To further examine the role of Mcl-1 in apoptosis of virus-infected BHK-21 cells, we tested whether siRNA Mcl-1 knock-down would result in increased apoptosis. Mcl-1 expression was inhibited by $\geq$90% with Mcl-1-specific siRNAs as determined by immunoblotting (Figure 3A,B) in experiments where transfection efficiency was ~90% (not shown). A representative FACS analysis of four experiments revealed a significant increase ($p < 0.048$) in apoptotic cell death in BeAn virus-infected cells transfected with Mcl-1-specific compared to scrambled siRNAs (Figure 3C). Analysis of viral replication in BHK-21 cells with siRNA knocked-down expression of Mcl-1 revealed a ~100-fold reduction in viral titers (Figure 3D), indicating that apoptosis inhibited BeAn viral replication. siRNA knock-down of Bcl-xL expression also resulted in a substantial increase in apoptosis (Figure 3E), indicating that Bcl-xL may also play an anti-apoptotic role in infected BHK-21 cells.

To further study the effect of Mcl-1 knock-down on TMEV replication, 22 stable, puromycin-resistant BHK-21 clones were generated, and two clones (clones 8 and 10) showing the greatest decrease in Mcl-1 expression (Figure 4A) were infected with virus and assessed for apoptosis. Both clones showed increased levels of apoptosis at 6 and 8 h pi ($p < 0.05$) and levels were significantly higher at 10 h pi ($p = 0.02$) compared to infected parental cells (Figure 4B) in an assay based on nuclear morphology of attached cells because of cpe was not reliable $\geq$ 12 hr pi. BeAn infection of both clones resulted in PARP, caspase -9 and caspase-3 cleavage (shown for clone 10 in Figure 4C) but not caspase-8 cleavage at 6 to 10 hr pi, suggesting that TMEV infection in BHK-21 cells activates the

intrinsic signaling pathway similar to its action in murine mϕs (13, 27). A caspase activity assay using a commercial luminescent reagent revealed a ~3-fold activation of caspase-9 (3-fold) as compared to ~1.7-fold for caspase-8 ($p = 0.01$) (Figure 4D); however, the increases in caspase activity were not robust probably because of the limited extent of apoptosis. In contrast to the immunoblotting results, knock-down of Mcl-1 did not lead to significantly increased initiator caspase activity (Figure 4D).

Temporal analysis of virus titers in infected parental and Mcl-1 knock-down cells, indicated a shortened virus growth curse for infected clone 10 cells, peaking at 8 to 10 h pi and resulting in 90% reduction in infectious viral yields as compared with viral kinetics ihn parental cells (Figure 5A). Northern blot analysis to determine whether the kinetics of single-stranded viral RNA (ss viral RNA) replication was also affected revealed no significant differences between parental and knock-down cells (Figure 5B). Pulse-chase analysis at 5 h pi indicated no differences in viral protein synthesis and polyprotein processing (Figure 5C). These results indicate that Mcl-1 is an essential pro-survival factor that enables increased infectious virus yields by inhibiting apoptosis and by its impact on a step in the viral life cycle later than viral RNA replication, protein synthesis, or polyprotein processing.

Early activation of p53 in infected BHK-21 cells. Mcl-1 expression is regulated by a variety of cytokines and growth factors through a number of signaling pathways (2, 13). Mcl-1 is also regulated by the p53 tumor suppressor protein (11), whose activation is required for the induction of apoptosis in BeAn virus-infected M1-D mϕs (28). Immunoblotting to determine whether p53 was also activated in infected BHK-21 cells

increased p53 expression as early as 15 min pi (Figure 6A). Ser-15 and Ser-20, two common p53 phosphorylation sites that are induced in BeAn-infected M1-D cells (28), did not differ in phosphorylation levels (not shown), suggesting that p53 may be activated by phosphorylation at other sites. Immunoblot analysis of immunoprecipitated p53 with monoclonal antibody to phospho-Ser, -Tyr and -Thr residues showed that p53 was phosphorylated in infected BHK-21 cells but not in BHK-21 cells incubated with UV-inactivated virus (Figure 6B). Similar analysis of the BH3-only pro-apoptotic proteins Noxa and Puma which are transcriptionally up-regulated by p53 (10, 11, 32) and activated in BeAn-infected M1-D mϕs (28), revealed up-regulation of only Noxa in infected BHK-21 cells (Figure 6C). Immunoblotting analysis for Bax and Bak expression showed increased expression and activation of only Bax (Figure 7D; Bak data not shown) at 30 min pi. These data demonstrate the close similarity of the apoptotic cell death pathway in BHK-21 cells and M1-D mϕs.

BeAn infection induces necrosis in N20.1 oligodendrocytes. Unlike the restricted infection of mϕs, infection of oligodendrocytes in mice appears to be highly productive (3). Analysis of cell death in the murine oligodendrocyte cell line N20.1 which is productively infected (30), showed a temporal profile similar to that in BHK-21 cells (Figure 7A); however, FACS analysis of PI- and Annexin V-stained cells indicated that essentially all of the cells underwent necrosis (Figure 7B). As expected, virus infection of both cell lines resulted in one-step growth kinetics with similar high viral yields (Figure 8C). Immunoblotting to examine the expression profile of the Bcl-2 anti-apoptotic proteins in BHK-21, N20.1 and M1-D cells showed high levels of Mcl-1 only in BHK-21 cells, with just detectable levels in N20.1 and M1-D cells (Figure 8C). Bcl-w was expressed at high levels

in N20.1 cells, suggesting that Bcl-w may be a critical pro-survival protein in oligodendrocytes; however, siRNA knock-down of Bcl-w did not result in increased apoptosis (not shown).

DISCUSSION

The mode of virus-induced cell death is critical in determining the host range of a virus, i.e., the extent of virus production and viral spread in an animal host and dissemination to other animal hosts. In picornavirus infections where rapid viral replication kinetics predominate, necrosis has generally been associated with productive infections while apoptosis is associated restricted infections (1, 6, 12, 14, 18, 29). TMEV infection has been shown to induce necrosis in rodent cells, such as BHK-21 and L929 cells, in association with high viral yields (14, 27), whereas murine mϕs undergo apoptosis exclusively, with interruption of virus production and decreased yields of infectious virus progeny. An in-depth characterization of infection in BHK-21 cells has not been carried out and the mechanism by which TMEV induces host-specific cell death to affect viral yields is not well understood. In the present study, we examined the mode of BeAn virus-induced cell death in BHK-21 cells, the role of Bcl-2 family pro-survival proteins, particularly Mcl-1, in regulating cell death, and the effect of apoptosis and necrosis on TMEV replication.

Our studies revealed apoptosis of only a minority of BHK-21 virus-infected cells (~20%), while a majority waS PI-positive (~60%) and underwent necrosis (Figure 1). The Bcl-2 multidomain, anti-apoptotic protein Mcl-1 was highly expressed in BHK-21 cells, with a decrease in expression at 10 to 12 h pi, consistent with the onset of apoptosis. siRNA knock-down of Mcl-1 resulted in a ~3-fold increase in apoptosis (Figures 2 and 3), indicating that Mcl-1 is important in regulating apoptosis in BHK-21 cells. Bcl-xL was also expressed at high levels (Figure 2D) and when knocked down by siRNAs, led to a similar increase in apoptosis (Figure 3E). Knock-down of both Mcl-1 and Bcl-xL did not result a in greater percentage of apoptotic cells than either pro-survival molecule alone (not shown), possibly

because either Mcl-1 or Bcl-xL is sufficient to counter most of the pro-apoptotic activity of Bax.

The apoptotic program that switched on at the time of exponential TMEV replication in BHK-21 cells was similar to that M1-D mϕs (27, 28), with hallmarks of activation of the intrinsic apoptotic pathway in a tumor suppressor protein p53-dependent manner (Figure 6A,B). Experiments in which Mcl-1 was stably knocked down to increase the otherwise low level of apopotsis in parental BHK-21 cells suggested that the subsequent activation of the Bcl-2 BH-only pro-apoptotic Noxa protein led to degradation of Mcl-1 (Figure 6C,D), activation of Bax, and, after the release of cytochrome c into the cytoplasm (not shown), cleavage of caspases-9 and-3 (Figure 4C). The early activation of Bax, in contrast to its later activation in infected M1-D cells, was surprising, but might be explained by the direct interaction of Bax with p53 inducing its homo-oligomerization and activation (8).

Analysis of one-step viral growth kinetics in Mcl-1 knock-down BHK-21 cells demonstrated a peak in viral growth at 8 to 10 h pi (~2 h earlier than in parental cells), leading to 90% reduction in infectious viral yields at 24 h pi (Figure 5A). While finding that viral RNA replication, protein synthesis, and polyprotein processing did not differ between parental cells and stable Mcl-1 knock-down cells (Figure 5B,C) pointed to a defect in virion assembly possibly due to damage from activated caspases, our preliminary experiments provide no evidence of differences in the assembly of 5S protomers and 14S pentamers (assembly intermediates) or in 150S mature virions in cells with stable knock-down of Mcl-1. Recently, Bryant and Clem (5) reported that a p35 mutant of *Autographa californica* multiple nucleopolyhedrovirus, a baculovirus that infects lepidopteran insects, did not induce

apoptosis despite caspase activity but did produce progeny virus with defects in stability and infectivity. This defect was rescued in the producer cells when virus was grown in the presence of zVAD-fmk (5). Studies are in progress to identify such a defect in TMEV virions grown in BHK-21 cells with stable knock-down of Mcl-1.

During persistent infection in the mouse CNS TMEV replication is observed primarily in mϕs (19, 22, 26) and to a lesser extent, in oligodendrocytes (3, 24). Blakemore et al. (3) found paracrystalline arrays of virions in oligodendrocytes by electron microscopy in chronically infected spinal cords, indicating that oligodendrocytes are productively infected and probably undergo necrosis. However, Tsunoda et al. (31) detected some TUNEL-positive oligodendrocytes in mice chronically infected with another low-neurovirulence TMEV, DA virus. Our *in vitro* analysis using the N20.1 oligodendrocyte cell line showed that infection with BeAn virus led to necrosis with the production of high viral titers, similar to BHK-21 cells. N20.1 oligodendrocytes expressed high levels of another Bcl-2 anti-apoptotic family protein, Bcl-w (Figure 7D) which is highly expressed in brain and spinal cord tissues (21, 21a), in neurons and glia (21). The lack of an effect of Bcl-w knock-down in N20.1 oligodendrocytes might rest in the robustness of the necrotic response to BeAn virus infection, such that the pro-survival activity of Bcl-w was not required. Further studies of primary murine oligodendrocytes and other murine oligodendrocyte cells lines are needed.

Acknowledgements

We thank Patricia Kallio for expert technical help, Robert P. Becker for electron microscopic analysis, and Shannon Hertzler and Zhiguo Liang for other aspects of the research. This work was supported by NIH grant NS065945 and the Modestus Bauer Foundation.

LITERATURE CITED

1. Agol, V. I., G. A. Belov, K. Bienz, D. Egger, M. S. Kolesnikova, N. T. Raikhlin, L. I. Romanova, E. A. Smirnova, and E. A. Tolskaya. 1998. Two types of death of poliovirus-infected cells: caspase involvement in the apoptosis but not cytopathic effect. Virology 252:343-353.
2. Akgul, C. 2009. Mcl-1 is a potential therapeutic target in multple types of cancer. Cell. Mol. Life Sci. 66:1326-1336.
3. Blakemore, W. F., C. J. Welsh, P. Tonks, and A. A. Nash. 1988. Observations on demyelinating lesions induced by Theiler's virus in CBA mice. Acta Neuropathol. (Berl). 76:581-589.
4. Brahic, M., J. F. Bureau, and T. Michiels. 2005. The genetics of the persistent infection and demyelinating disease caused by Theiler's virus. Annu. Rev. Microbiol. 59:279-298.
5. Bryant, B., and R. J. Clem. 2009. Caspase inhibitor p35 is required for the production of robust baculovirus virions in Trichoplusia ni TN-368 cells. J. Gen. Virol. 90:654-661.
6. Carthy, C. M., D. J. Granville, K. A. Watson, D. R. Anderson, J. E. Wilson, D. Yang, D. W. Hunt, and B. M. McManus. 1998. Caspase activation and specific cleavage of substrates after Coxsackievirus B3-induced cytopathic effect in HeLa cells. J. Virol. 72:7669-7675.
7. Chao, J. R., J.-M. Wang, S.-F. Lee, H.-W. Peng, Y.-H. Lin, C.-H. Chou, J.-C. Li, H.-M. Huang, C.-K. Chou, M.-L. Kuo, J. J.-Y. Yen, and H.-F. Yang-Yen. 1998. mcl-1 is an immediate-early gene activated by the granulocyte-macrophage colong-stimulating factor (GM-CSF) signaling pathway and is one component of the GM-CSF viability response. Mol. Cell. Biol. 18:4883-4898.

8. Chipuk, J. E., T. Kuwana, L. B. Bouchier-Hayers, N. M. Droin, D. D. Newmeyer, M. Schuler, and D. R. Green. 2004. Direct activation of Bax by p53 mediates mitochondrial membrane permeabilization and apoptosis. Science 303:1010-1014.

9. Fiers, W., R. Beyeart, W. Declercq, and P. Vandenabeele. 1999. More than one way to die: necrosis and reactive oxygen damage. Oncogene 18:7719-7730.

10. Fischer, S. F., G. T. Belz, and A. Strasser. 2008. BH3-only protein Puma contributes to death of antigen-specific T cells during shutdown of an immune response to acute viral infection. Proc. Natl. Acad. Sci. U.S.A. 105:3035-3040.

11. Haupt, S., M. Berger, Z. Goldberg, and Y. Haupt. 2003. Apoptosis - the p53 network. J. Cell Sci. 116:4077-4085.

12. Henke, A., H. Launhardt, K. Klement, A. Stelzner, R. Zell, and T. Munder. 2000. Apoptosis in Coxsackie B3-caused diseases: interaction between the capsid protein VP2 and the proapoptotic protein siva. J. Virol. 74:4284-4290.

13. Jelachich, M. L., C. Brumlage, and H. L. Lipton. 1999. Differentiation of M1 myeloid precursor cells into macrophages results in binding and infection by Theiler's murine encephalomyelitis virus (TMEV) and apoptosis. J. Virol. 73:3227-3235.

14. Jelachich, M. L., and H. L. Lipton. 1996. Theiler's murine encephalomyelitis virus kills restrictive but not permissive cells by apoptosis. J. Virol. 70:6856-6861.

15. Jelachich, M. L., H. V. Reddi, M. Trottier, B. P. Schlitt, and H. L. Lipton. 2004. Susceptibility of peritoneal macrophages to infection by Theiler's virus. Virus Res. 104:123-127.

16. Kobayashi, S., S.-H. Lee, X. W. Meng, J. L. Mott, S. F. Bronk, N. W. Werneburg, R. W. Craig, S. H. Kaufman, and G. J. Gores. 2007. Serine 64 phosphorylation enhances the antiapoptotic function of Mcl-1. J. Biol. Chem. 282:18407-18417.

17. Kozopas, K. M., T. Yang, H. L. Buchan, P. Zhou, and R. W. Craig. 1993. MCL 1, a gene expressed in programmed myeloid cell differentiation, has sequence similarity to BCL2. Proc. Natl. Acad. Sci. U. S. A. 90:3516-3520.

18. Kuo, R.-L., S.-H. Kung, Y.-Y. Hsu, and W.-T. Liu. 2002. Infection of enterovirus 71 or expression of its 2A protease induces apoptotic cell death. J. Gen. Virol. 83:1367-1376.

19. Lipton, H. L., G. Twaddle, and M. L. Jelachich. 1995. The predominant virus antigen burden is present in macrophages in Theiler's murine encephalomyelitis virus (TMEV)-induced demyelinating disease. J. Virol. 69:2525-2533.

20. Liu, H., H. Perlman, L. J. Pagliari, and R. M. Pope. 2001. Constitutively activated Akt-1 is vital for the survival of human monocyte-differentiated macrophages: Role of Mcl-1, independent of nuclear factor (NF)-kB, Bad, or caspase activation. J. Exp. Med. 194:113-125.

21. Minami, M., K. L. Jin, W. Li, T. Nagayama, D. C. Henshall, and R. P. Simon. 2000. Bcl-w expression is increased in brain regions affected by focal cerebral ischemia in the rat. Neurosci. Lett. 279:193-195.

21a O'Reilly, L.A., C. Print, G.Hauseman, K. Morishi, S. Cory, D. C. Huang, A. Strasser. Tissue expression and subcellular localization of the pro-survival molecule Bcl-w. Cell Death Differ. 8:486-494.

22. Pena-Rossi, C., M. Delcroix, I. Huitinga, A. McAllister, N. van Rooijen, E. Claassen, and M. Brahic. 1997. Role of macrophages during Theiler's virus infection. J. Virol. 71:3336-3340.

23. Reed, L. J., and H. A. Muench. 1938. A simple method of estimating fifty percent endpoints. Am. J. Hygiene 27:493-497.

24. Rodriguez, M., J. L. Leibowitz, and P. W. Lampert. 1983. Persistent infection of oligodendrocytes in Theiler's virus-induced demyelination. Ann. Neurol. 13:426-433.

25. Rozhon, E. J., J. D. Kratochvil, and H. L. Lipton. 1983. Analysis of genetic variation in Theiler's virus during persistent infection in the mouse central nervous system. Virology 128:16-32.

26. Schlitt, B. P., M. Felrice, M. L. Jelachich, and H. L. Lipton. 2003. Apoptotic cells, including macrophages, are prominent in Theiler's virus-induced inflammatory, demyelinating lesions. J. Virol. 77:4383-4388.

27. Son, K.-N., R. P. Becker, P. Kallio, and H. L. Lipton. 2008. Theiler's virus-induced apoptosis in M1-D macrophages is Bax-mediated through the mitochondrial pathway, resulting in loss of infectious virus: A model for persistence in the mouse central nervous system. J. Virol. 82:4502-4510.

28. Son, K.-N., S. Pugazhenthi, and H. L. Lipton. 2009. Activation of tumor suppressor protein p53 is required for Theiler's murine encephalomyelitis virus-induced apoptosis in M1-D macrophages. J. Virol. 83:10770-10777.

29. Tolskaya, E. A., L. I. Romanova, M. S. Kolesnickova, T. A. Ivannikova, E. A. Smirnova, N. T. Raikhlin, and V. I. Agol. 1995. Apoptosis-inducing and apoptosis-preventing functions of poliovirus. J. Virol. 69:1181-1189.

30. Trottier, M., P. Kallio, W. Wang, and H. L. Lipton. 2001. High numbers of viral RNA copies in the central nervous system of mice during persistent infection with Theiler's virus. J. Virol. 75:7428.

31. Tsunoda, I., C. I. B. Kurtz, and R. S. Fujinami. 1997. Apoptosis in acute and chronic central nervous system disease induced by Theiler's murine encephalomyelitis virus. Virology 228:388-393.

32. Villunger, A., E. M. Michalak, L. Coultas, F. Mullauer, G. Bock, M. J. Ausserlechner, J. M. Adams, and A. Strasser. 2003. p53- and drug-induced apoptotic responses mediated by BH3-only proteins Puma and Noxa. Science 302:1036-1038.

33. Zhou, P., L. Quian, K. M. Kozopas, and R. W. Craig. 1997. Mcl-1, a Bcl-2 family member, delays the death of hematopoietic cells under a variety of apoptosis-inducing conditions. Blood 89:630-643.

FIGURE LEGENDS

Figure 1. BeAn virus infection of BHK-21 cells (moi = 10) led primarily to necrosis, with a minority of cells undergoing apoptosis. (A) Representative WST-1 cell survival assay revealed progressive cell death to 40 h pi; error bars = sd. (B) FACS analysis of PI- and Annexin V-stained cells showing a temporal profile of PI-positive cells, probably necrotic (majority of cells; upper quadrants) and apoptotic cells (minority of cells; lower right quadrant). (C) FACS analysis showing that infected cells develop high levels of reactive oxygen species (ROS) at 10-12 h pi. (D) Electron microscopy of infected BHK-21 cells showing a relatively normal-appearing cell prior to onset of apoptosis at 8 h pi (left), a necrotic cell at 16 h pi, appearing swollen with little recognizable cytoplasmic or nuclear architecture (center); and an apoptotic cell at 16 h pi, appearing mildly shrunken, with condensed nuclear chromatin and blebbing of part of its nucleus, and perinuclear proliferating membranes representing viroplasm ("viral factory") (right).

Figure 2. Expression profile of Bcl-2 family anti-apoptotic members determined by immunoblotting. (A) Mcl-1 expression in five mouse mϕ cell lines, mouse L929 and MEF fibroblasts, and Syrian hamster BHK-21 cells. (B) Comparison of the expression of the five Bcl-2 family anti-apoptotic proteins in BHK-21 and M1-D mϕs, not the abundant Bcl-xL and Mcl-1 expression in BHK-21 cells. (C) Loss of Mcl-1 expression in BHK-21 cells grown in 0.1% FBS for 24 and 36 h. (D) Expression of Bcl-2 anti-apoptotic proteins in BeAn virus-infected BHK-21 cells (moi = 10) at the indicated times pi; the substantial reduction of Mcl-1 levels at 10 to 12 h pi is consistent with the induction of apoptosis at this time. (E)

Densitometric analysis of Bcl-xL and Mcl-1 immunoblot data in infected BHK-21 cells over time pi normalized to βactin.

Figure 3. siRNA knock-down demonstrates an anti-apoptotic role of Mcl-1 and Bcl-xL in BeAn virus-infected BHK-21 cells. (A) Timeline of cell death analysis in siRNA experiments. (B) Immunoblot analysis revealing 90% knock down of the amount of Mcl-1 with specific compared to scrambled siRNAs. (C) Representative FACS analysis of PI- and Annexin V-stained cells revealed an ~3-fold increase in apoptotic cells (right lower quadrant) after infection of Mcl-1 knock-down cells at 16 h pi. (D) Infectious virus yields of Mcl-1 siRNA-transfected cells was significantly decreased at 16 h pi ($P < 0.01$) compared to viral yields of scrambled siRNA-transfected cells; error bars = sd. (E) FACS analysis of PI- and Annexin V-stained cells demonstrated that both Mcl-1 and Bcl-xL function as anti-apoptotic proteins in infected BHK-21 cells.

Figure 4. BeAn virus infection of BHK-21 cells with stable Mcl-1 knock-down induces apoptosis through the intrinsic pathway. (A) Two stable Mcl-1 knock-down clones (clones 8 and 10) showed a 90% reduction in Mcl-1 expression. (B) BeAn infection (moi = 10) of clones 8 and 10 induced apoptosis beginning at 6 h pi as assessed based on nuclear morphology (DAPI staining) (error bars = sd). (C) Immunoblot analysis revealed PARP and caspases-9 and -3 cleavage in infected Mcl-1 knock-down cells (shown for clone 10) at 8 and 10 h pi. (D) Activation of caspase-9 but not caspase-8 over time in a Luc assay of parental and Mcl-1 knock-down BHK-21 cells (error bars = SE).

Figure 5. Stable Mcl-1 knock-down in BHK-21 cells does not affect viral RNA synthesis or translation but reduces infectious virus production of compared to parental cells. (A) Temporal kinetics of BeAn infection showing that peak virus titers in knock-down cells were significantly reduced at 8-12 h pi compared to parental cells ($p = 0.04$ at 12 h; error bars = sd). (B) Northern blot analysis showing similar replication of ss viral RNA in both parental and knock-down cell lines. (C) Cells lines pulsed with [^{35}S]methione at 5.5 h pi for 5 min followed by chases at indicated times revealed similar protein synthesis, including polyprotein processing into the final structural and nonstructural viral proteins (labeled on the right).

Figure 6. BeAn virus-infected parental BHK-21 cells show p53 and Noxa activation upstream and Bax downstream of Mcl-1. (A) Immunoblot analysis showing after infection (moi = 10) of parental BHK-21 cells detectable p53 from 15 to 240 min pi but not in mock-infected cells (later not shown). (B) Immunoblot of p53 immunoprecipitated from infected cells early pi and incubated with mouse monoclonal antibody to phosphoserine/ threonine/tyrosine demonstrated phosphorylation of p53 at 60 and 120 min pi, whereas control, parental BHK-21 cells infected with UV-inactivated BeAn virus showed no p53phosphorylation. (C and D) Immunoblots showing that BeAn infection leads to activation of Noxa, but not Puma at 8 to 10 h and to activation of Bax at 30 min pi and increased amounts of total Bax (D).

Figure 7. BeAn virus-induced necrosis in N20.1 oligodendrocyte cells. (A) Comparison of the temporal profile of virus induced-cell death of N20.1 and parental BHK-21 cells in a

representative experiment using the Wst-1 assay; error bars = sd. (B) BeAn virus infection of N20.1 cells resulted primarily in necrotic cell death; 42% of cells stained PI-positive by 12 h pi, whereas only 4% underwent apoptosis. (C) Comparison of one-step growth kinetics of BeAn virus in N20.1 and BHK-21 cells showed similar peaks of high virus titers by 12-14 h pi; error bars = sd . (D) Immunoblot analysis of the five Bcl-2 family anti-apoptotic proteins showed that Bcl-w was highly expressed in the N20.1 oligodendrocytes compared to BHK-21 and M1-D cells. The low expression level of Mcl-1 in M1-D cells was not detected in this immunoblot.

Figure 1

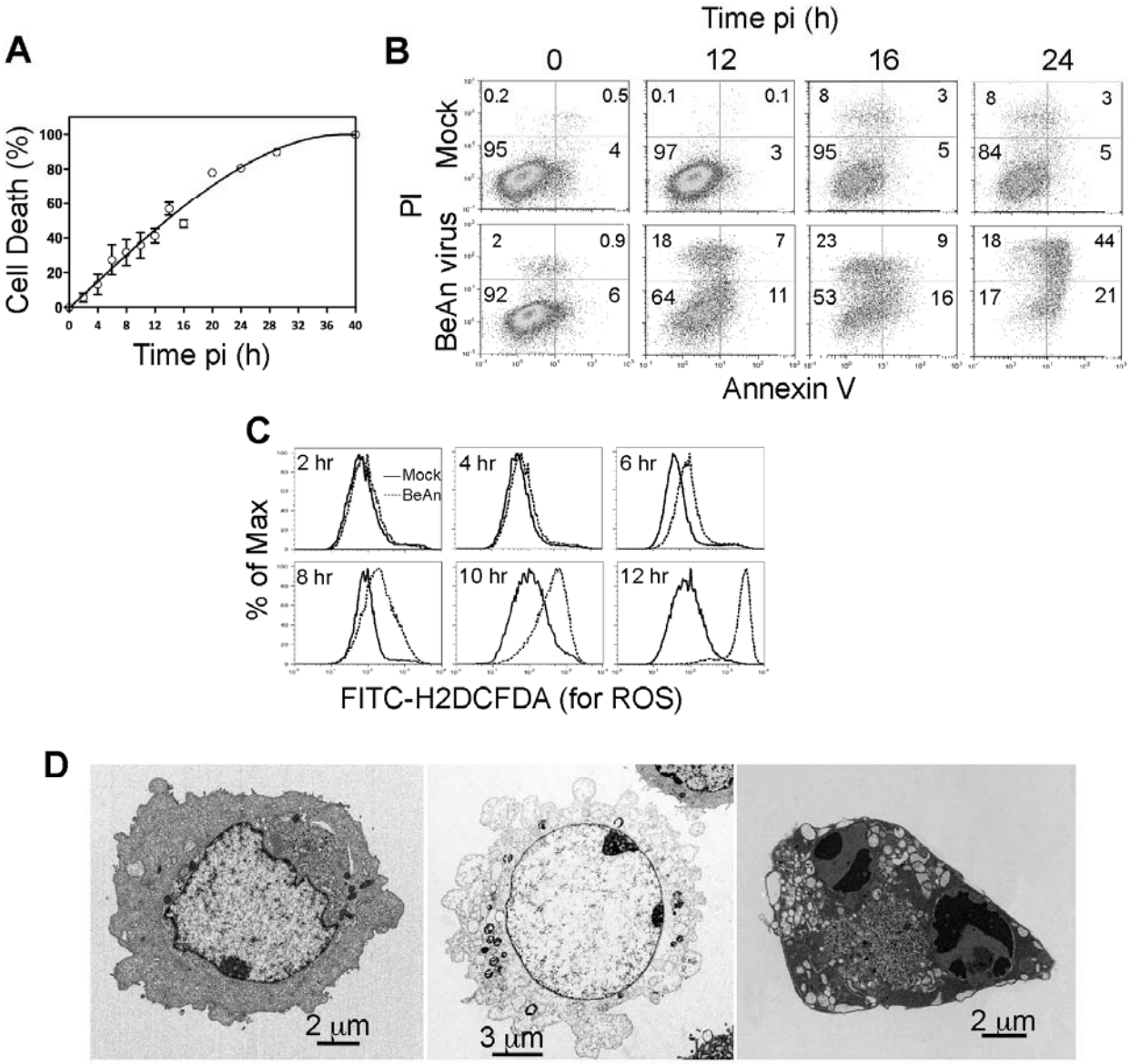
A
Cell Death (%)
Time pi (h)
B
Time pi (h)
0
12
16
24
Mock
BeAn virus
PI
Annexin V
C
2 hr
4 hr
6 hr
8 hr
10 hr
12 hr
Mock
BeAn
% of Max
FITC-H2DCFDA (for ROS)
D
2 μm
3 μm
2 μm

Figure 2

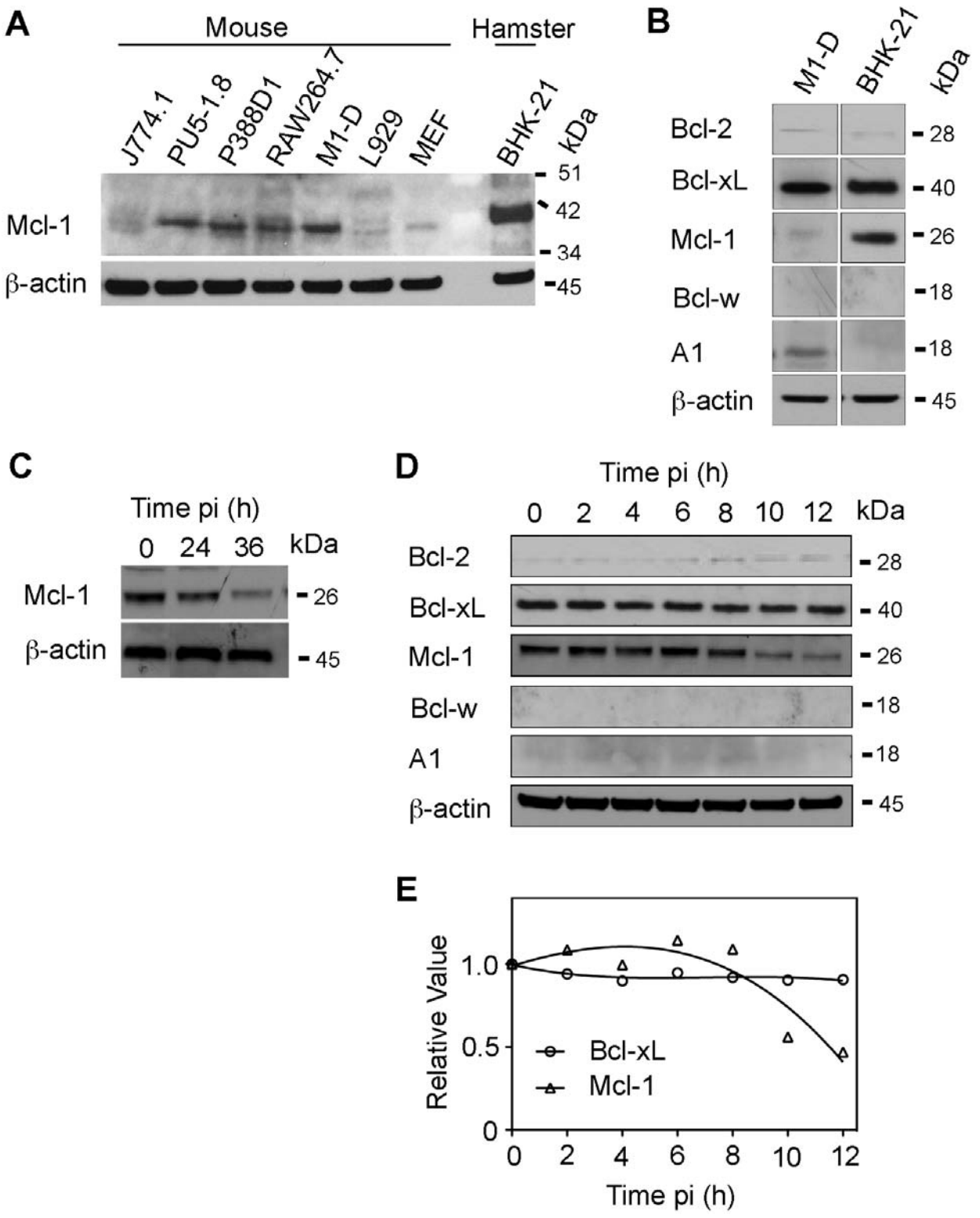
A
Mouse
Hamster
J774.1
PU5-1.8
P388D1
RAW264.7
M1-D
L929
MEF
BHK-21
kDa
Mcl-1
β-actin
51
42
34
45
B
M1-D
BHK-21
kDa
Bcl-2
Bcl-xL
Mcl-1
Bcl-w
A1
β-actin
28
40
26
18
18
45
C
Time pi (h)
0 24 36 kDa
Mcl-1
β-actin
26
45
D
Time pi (h)
0 2 4 6 8 10 12 kDa
Bcl-2
Bcl-xL
Mcl-1
Bcl-w
A1
β-actin
28
40
26
18
18
45
E
Relative Value
1.0
0.5
0
Bcl-xL
Mcl-1
0 2 4 6 8 10 12
Time pi (h)

Figure 3

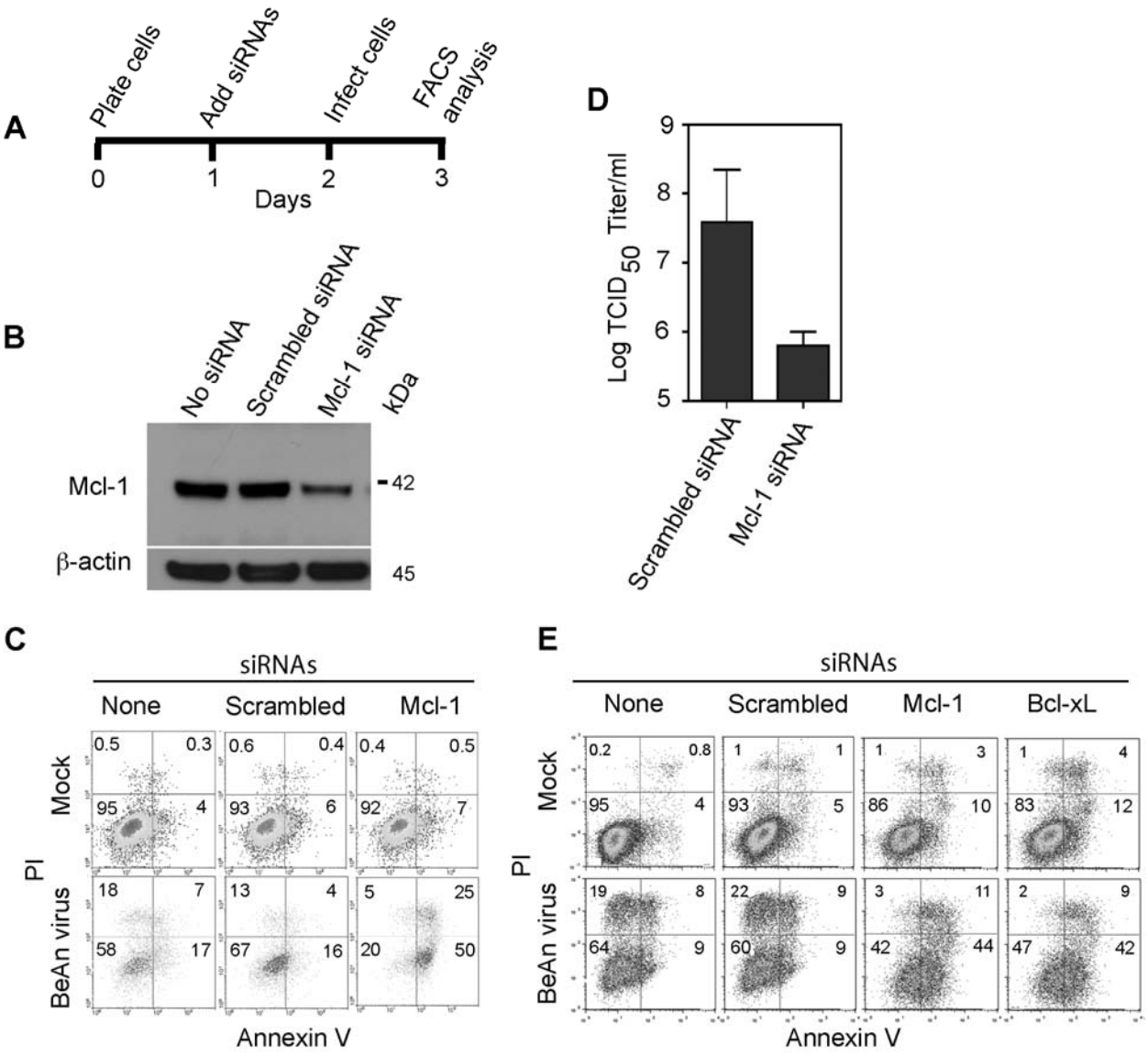
A
Plate cells
Add siRNAs
Infect cells
FACS analysis
0
1
2
3
Days
B
No siRNA
Scrambled siRNA
Mcl-1 siRNA
kDa
Mcl-1
42
β-actin
45
D
Log TCID50 Titer/ml
9
8
7
6
5
Scrambled siRNA
Mcl-1 siRNA
C
siRNAs
None
Scrambled
Mcl-1
Mock
BeAn virus
PI
0.5
0.3
0.6
0.4
0.4
0.5
95
4
93
6
92
7
18
7
13
4
5
25
58
17
67
16
20
50
Annexin V
E
siRNAs
None
Scrambled
Mcl-1
Bcl-xL
Mock
BeAn virus
PI
0.2
0.8
1
1
1
3
1
4
95
4
93
5
86
10
83
12
19
8
22
9
3
11
2
9
64
9
60
9
42
44
47
42
Annexin V

Figure 4

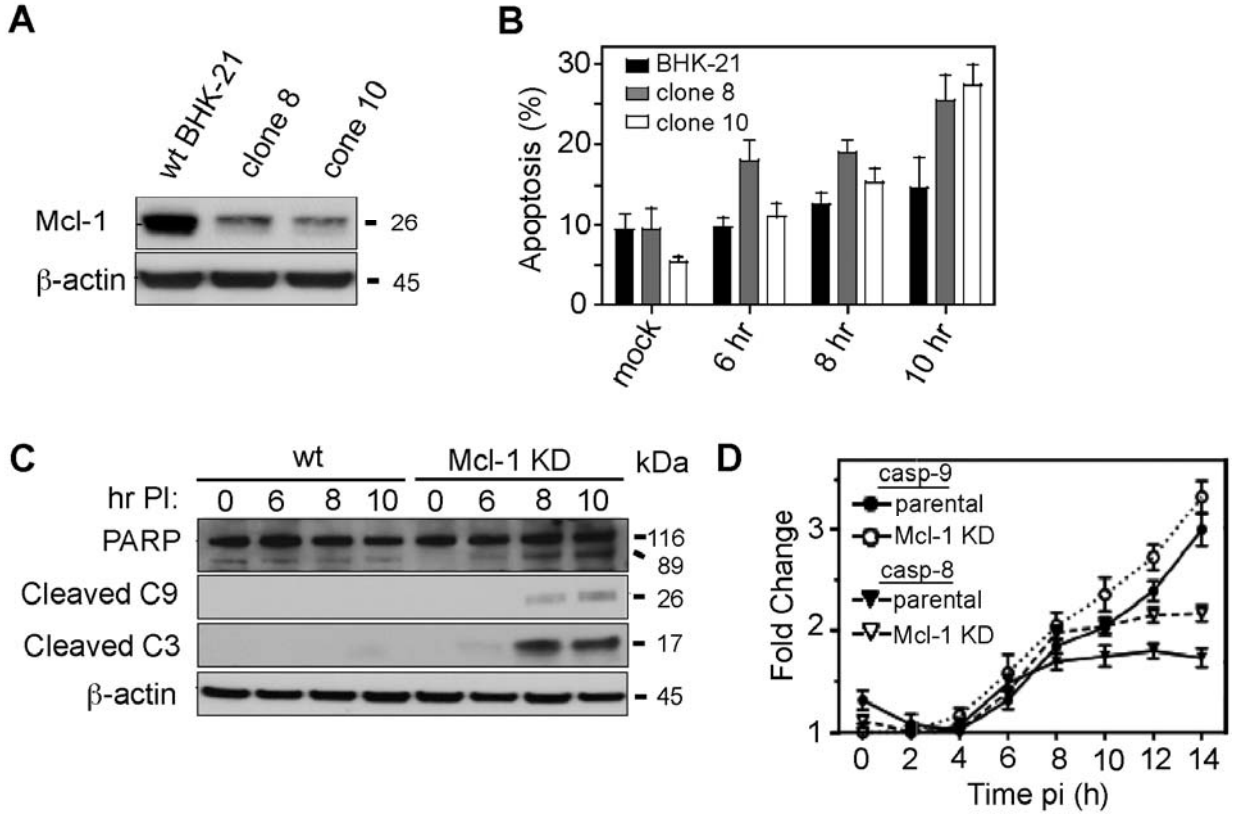
A
wt BHK-21
clone 8
cone 10
Mcl-1
β-actin
26
45
B
BHK-21
clone 8
clone 10
Apoptosis (%)
30
20
10
0
mock
6 hr
8 hr
10 hr
C
wt
Mcl-1 KD
kDa
hr PI:
0 6 8 10 0 6 8 10
PARP
Cleaved C9
Cleaved C3
β-actin
116
89
26
17
45
D
casp-9
parental
Mcl-1 KD
casp-8
parental
Mcl-1 KD
Fold Change
3
2
1
0 2 4 6 8 10 12 14
Time pi (h)

Figure 5

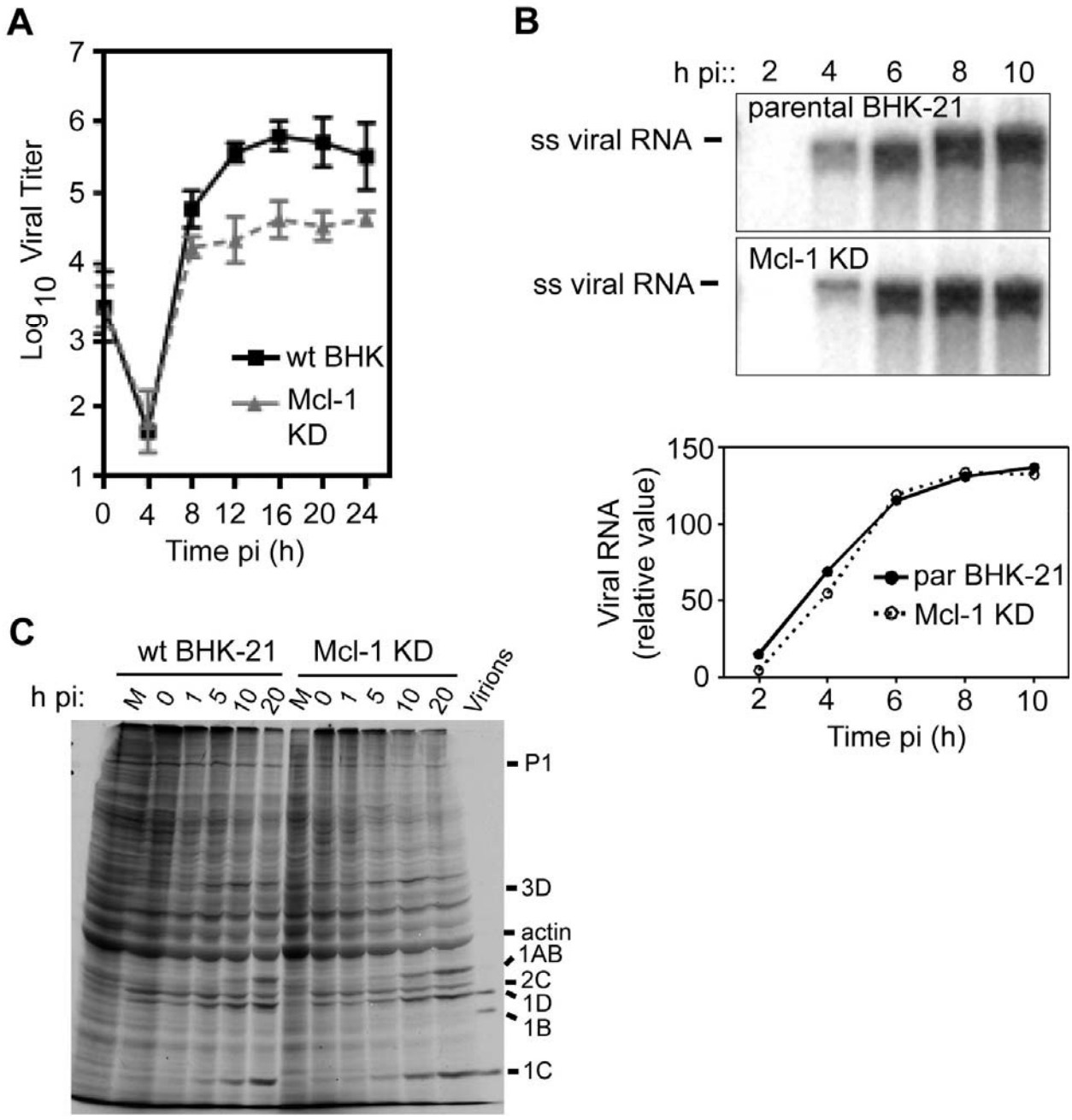
A
Log10 Viral Titer
Time pi (h)
wt BHK
Mcl-1 KD
B
h pi:: 2 4 6 8 10
parental BHK-21
ss viral RNA
Mcl-1 KD
ss viral RNA
Viral RNA (relative value)
par BHK-21
Mcl-1 KD
Time pi (h)
C
wt BHK-21
Mcl-1 KD
h pi:
M 0 1 5 10 20 M 0 1 5 10 20 Virions
P1
3D
actin
1AB
2C
1D
1B
1C

Figure 6

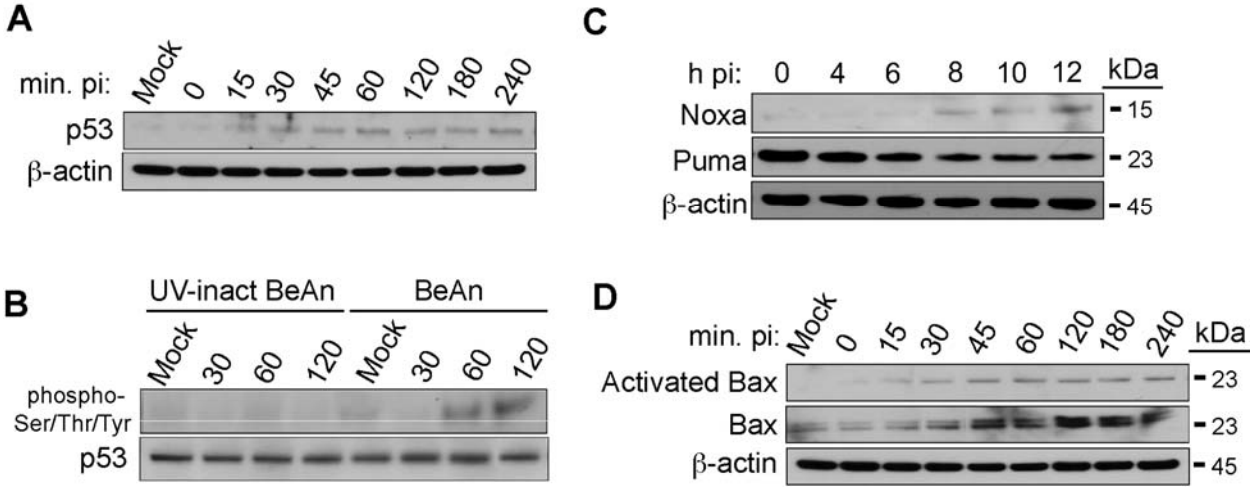
A
min. pi:
Mock
0
15
30
45
60
120
180
240
p53
β-actin
C
h pi:
0
4
6
8
10
12
kDa
Noxa
Puma
β-actin
15
23
45
B
UV-inact BeAn
BeAn
Mock
30
60
120
Mock
30
60
120
phospho-
Ser/Thr/Tyr
p53
D
min. pi:
Mock
0
15
30
45
60
120
180
240
kDa
Activated Bax
Bax
β-actin
23
23
45

Figure 7

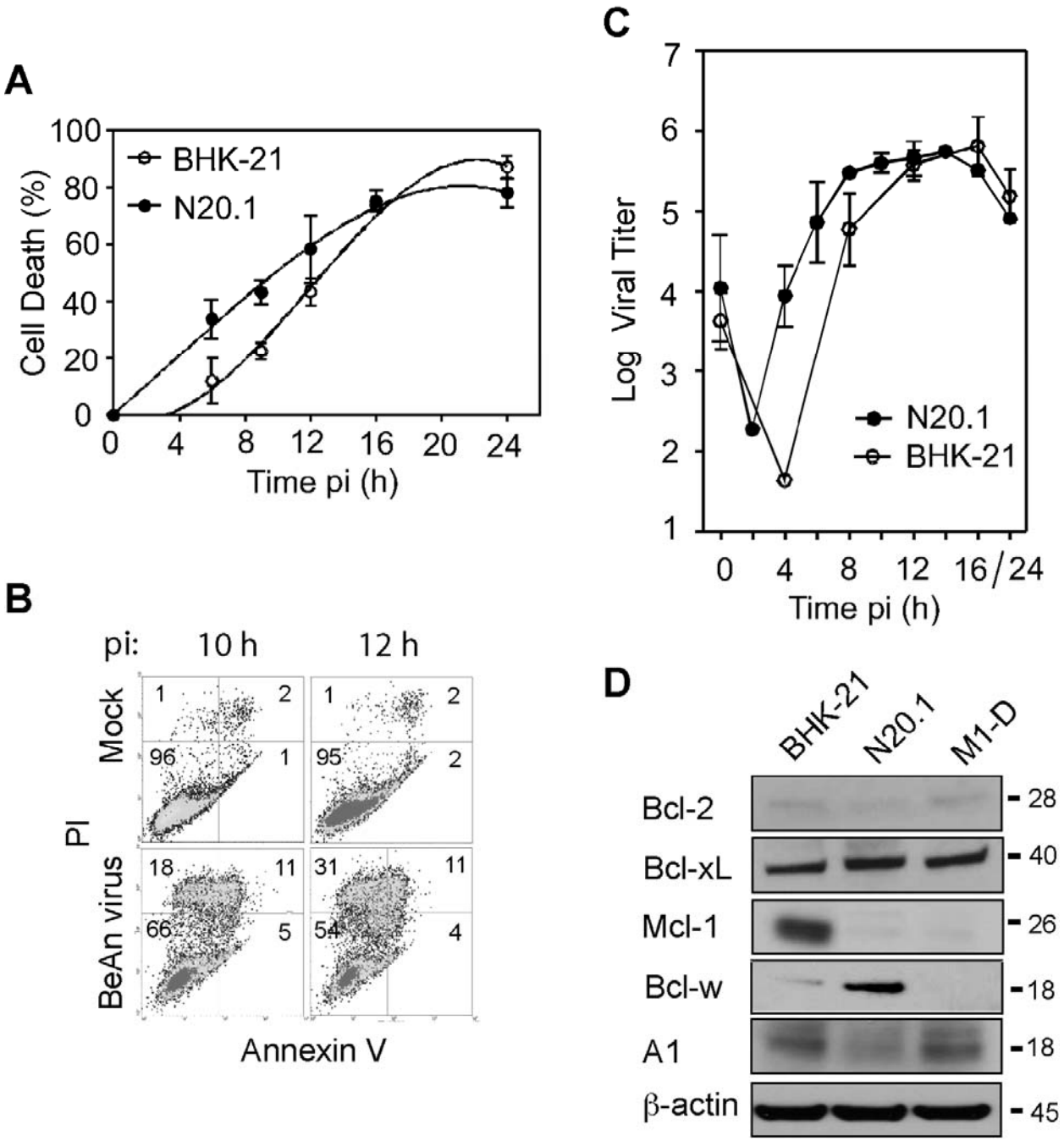
A
Cell Death (%)
Time pi (h)
BHK-21
N20.1
B
pi:
10 h
12 h
Mock
BeAn virus
PI
Annexin V
C
Log Viral Titer
Time pi (h)
N20.1
BHK-21
D
BHK-21
N20.1
M1-D
Bcl-2
Bcl-xL
Mcl-1
Bcl-w
A1
β-actin
28
40
26
18
18
45